Research Article

ADVANCED PHOTONICS

Extreme events in quantum cascade lasers

Olivier Spitz,[a,b,c,*] Jiagui Wu,[c,d] Andreas Herdt,[e] Grégory Maisons,[b] Mathieu Carras,[b] Wolfgang Elsäßer,[e] Chee-Wei Wong,[c] and Frédéric Grillot[a,c,f]

[a]LTCI, Télécom Paris, Institut Polytechnique de Paris, Palaiseau, France
[b]mirSense, Centre d'Intégration NanoInnov, Palaiseau, France
[c]University of California Los Angeles, Fang Lu Mesoscopic Optics and Quantum Electronics Laboratory, Los Angeles, California, United States
[d]Southwest University, College of Electronic and Information Engineering, Chongqing, China
[e]Technische Universität Darmstadt, Darmstadt, Germany
[f]University of New Mexico, Center for High Technology Materials, Albuquerque, New Mexico, United States

Abstract. We demonstrate experimentally that mid-infrared quantum cascade lasers (QCLs) operating under external optical feedback exhibit extreme pulses. These events can be triggered by adding small amplitude periodic modulation, with the highest success rate for the case of a pulse-up excitation. These findings broaden the potential applications for QCLs, which have already been proven to be a semiconductor laser of interest for spectroscopic applications and countermeasure systems. The ability to trigger extreme events paves the way for optical neuron-like systems where information propagates as a result of high intensity bursts.

Keywords: extreme pulses; quantum cascade lasers; nonlinear dynamics; mid-infrared photonics.

Received Aug. 16, 2019; revised manuscript received Sep. 5, 2020; accepted for publication Sep. 25, 2020; published online Oct. 21, 2020.

[DOI: 10.1117/1.AP.2.6.066001]

1 Introduction

The concept of extreme pulses is adapted to almost any kind of population. Those extreme events can be studied in a number of diversified fields, such as hydrodynamics,[1] electronic circuits,[2] climatology,[3] and epileptic crises.[4] More generally, extreme events, which also include freak waves or rogue waves, describe random isolated events with amplitudes well above those of neighboring ones, and which occur more often than expected from the distribution of lower amplitude events.[5] Research is carried out in various fields of science to report on their generation and to try to find a policy by which extreme events could possibly abide. In optics, extreme events have been studied from several viewpoints,[6] in varied configurations such as semiconductor lasers,[7] fiber lasers,[8] photonic crystals,[9] and microwave antennas.[10] On the other hand, theoretical work followed experimental demonstrations of optical extreme events,[11,12] providing different insights into the formation of these giant pulses. As opposed to strict rogue waves, extreme events can pop up through the variation of a controlled parameter, as it will be shown later on in this article. These extreme events can, for instance, take place in telecommunication data streams, where the emergence of high intensity peaks inside an optical fiber sets the limit of a high-speed optical communication link. Despite a plethora of studies dealing with extreme events driven by various mechanisms, an intensive and comprehensive investigation of the emergence of such extreme pulses in the mid-infrared field is still missing. Hence, it remains of prime importance to study them beforehand and understand their origins, in order to be able to better control them in future practical applications.[13] Experimentally, means of identifying extreme events vary with the type of dynamics studied. Several criteria are thus generally applied to the data, and the strictest one, leading to the identification of the lowest number of extreme events, should be used. To detect extreme events from experimental data, the probability density function (PDF) of an appropriate attribute of the data needs to be analyzed, and crest or wave heights are commonly used.[14] Once extracted from the data, heights are compared to a threshold value, above which events can be considered extreme. This threshold is generally defined as twice the significant height H_s of the dataset, which represents the average of the higher third of heights.[15] Another threshold widely used relies on the standard deviation (σ) and the mean value (μ) of the data, and an event is considered extreme if it exceeds $\mu + 8 \times \sigma$.[16] However, a criterion with a lower threshold ($\mu + 6 \times \sigma$ or even $\mu + 4 \times \sigma$) is also commonly

*Address all correspondence to Olivier Spitz, olivier.spitz@telecom-paris.fr

used without loss of generality.[17,18] This threshold alone is however not sufficient to identify extreme events, and it is necessary to verify that the PDFs represent long-tailed distributions. In this study, we use both thresholds because, on the one hand, the $\mu + 8 \times \sigma$ threshold is more restrictive, so we can ensure that we observe extreme events. On the other hand, the threshold related to H_s allows us to take into account more events so that we can display relevant statistics with enough data. The mechanism leading to the birth of such extreme events can be explained by an external crisis[19] triggered by an external parameter, as we will explain hereafter. The optical source generates a chaotic output, and the related bifurcation diagram is bounded because the system is stable. After the crisis, trajectories can explore a much larger region in the phase space, and the bifurcation diagram expands. This process creates pulses whose maxima are well above those usually found in the chaotic output. However, the large pulses must seldom occur, because as long as the extreme events are very rare, the average value of the intensity of the peaks and its variance remain similar to the values before the crisis. If the large events become the norm, the threshold for extreme events will subsequently increase and all the events will be considered as regular. This means that the bifurcation diagram becomes stable again, and the output displays chaos without extreme events. Given the fact that chaos and positive Lyapunov exponents have already been encountered in quantum cascade lasers (QCLs) under external optical feedback (OF),[20] it is not surprising to observe that these lasers can also be prone to extreme pulses. Despite that, it is clear that the formation of such events in QCLs can be further explained through strong numerical modeling, taking into account the peculiar characteristics of QCLs, in particular, the intersubband carriers dynamics and the transport properties.

This article aims at pushing further the concept of extreme events in semiconductor QCLs. Such lasers were experimentally demonstrated for the first time in 1994, under cryogenic temperatures.[21] Since then, they have experienced a fast development allowing them to be used in several industrial applications, up to room temperature, due to the large number of wavelengths QCLs can achieve.[22] QCLs emitting in the mid-infrared have been successfully used for countermeasure systems[23] and free-space communications,[24] whereas QCLs emitting in the THz domain are of prime interest for spectroscopy of explosives and drugs[25] and for real-time imaging.[26] The physics involved with mid-infrared QCLs is totally different than that in diode lasers. For instance, as opposed to the well-established diode lasers, QCLs are overdamped oscillators in which polarization and population inversion adiabatically follow the field, owing to the ultrashort carrier lifetime in the picosecond range. As the carrier lifetime is ~10 times smaller than the photon lifetime, the relaxation oscillations are well-suppressed, which is a peculiar feature of those unipolar lasers as opposed to their bipolar counterparts. In addition, the very sharp electronic transitions among the conduction-band states (subbands) lead to completely different selection rules and behaviors from those observed in diode lasers with interband transitions. The dipole moments, which determine the oscillator strengths for the transitions, are also of a different nature, hence resulting from the orthogonality of the envelope functions. Therefore, a wide range of studies have recently emerged in the literature, aiming at understanding their dynamical properties with the view to turn them into practical applications. For instance, controlling the QCL dynamics is of prime importance for a broad range of free-space applications, as the atmosphere is highly transparent between 3 and 5 μm and between 8 and 12 μm. Up to date, the nonlinear dynamics studies of mid-infrared QCLs under OF focused on deterministic chaos, both at room temperature[27] and cryogenic temperature.[20] This chaotic pattern is composed of intensity dropouts, called low-frequency fluctuations (LFFs), and experiments showed that an extensive control of these spikes was possible under a periodic excitation.[28] In this work, we experimentally build up a nonlinear dynamical setup to show the first extreme events emitted by a mid-infrared QCL operating under external feedback. In addition to that, we also describe several methods to trigger those events with a maximum success rate of 47%. We also show that all of the retrieved extreme events, even those which are not that tremendous, can be predicted and potentially suppressed before they occur due to a dip pattern in the structure of the temporal response. This is, to the best of our knowledge, the very first experimental demonstration of generation and control on extreme events in the mid-infrared field with semiconductor lasers. Although we do not mathematically prove that such extreme events are rogue, we use the aforementioned criteria to qualitatively interpret them. Thus, the amplitude of these extreme events is compared with both the abnormality $A = 2$ criterion (called C_1 in the following) and the most restrictive one, that is to say $\mu + 8 \times \sigma$ criterion (called C_2 in the following), in order to strengthen our claims.

Overall, this article brings new insights in the physics of QCLs, hence demonstrating their high potential for nonlinear science, such as the generation of mid-infrared extreme pulses. Indeed, quantum cascade emitters exhibit peculiar properties that can produce rich nonlinear dynamics and phase-coherent phenomena.[29,30] In QCLs, the nonlinear saturation of the intersubband transition plays a significant role in the dynamical properties related to the coupling of the different electromagnetic modes, which is also of first importance for phase coupling, pulse generation, and mode-locking. The latter can even be further enhanced when an OF configuration is applied to the laser. In addition to that, nonlinear saturation is also known to determine the steady-state output power and the laser response to fast modulation. Although this effect is naturally involved in diode lasers, it becomes more peculiar in QCLs due to the dephasing and gain relaxation times that are much shorter than the cavity roundtrip time. Therefore, the nonlinear saturation coefficient associated with intersubband transitions is expected to not only be ultrafast and broadband but also several orders of magnitude stronger than the optical nonlinearities in bulk semiconductors.[31,32] These extreme events can be triggered through the addition of a small-amplitude periodic modulation, with the highest success rate for the case of a pulse-up excitation, in agreement with simulations with other semiconductor lasers. In addition, understanding the origin of such extreme events and how to control them is of vital importance for the development of secure transmission lines using mid-infrared QCLs. Indeed, the atmospheric turbulence on the propagation path is known to be less significant at higher wavelengths.[33] In the latter case, extreme events can also be used to disrupt a data transmission link for modern and future free-space optical transmission lines. Last, but not least, we can envision applying those results in neuromorphic clusters composed of optical neurons able to communicate due to sudden and sharp bursts.

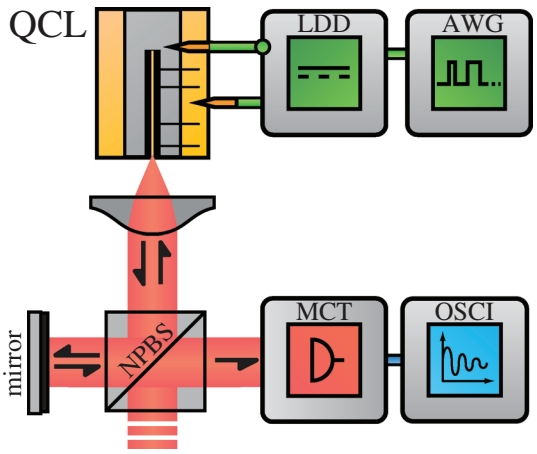

Fig. 1 Experimental setup with an external cavity for the OF via a mirror. NPBS, nonpolarizing beam splitter; MCT, mercury–cadmium–telluride detector; OSCI, fast oscilloscope; AWG, arbitrary waveform generator; LDD, laser diode driver.

2 Methods

Most of the experiments and numerical works studying extreme events in semiconductor lasers focus on an optical injection scheme.[18,34–39] VCSELs and laser diodes are the most common devices in these experiments because they are renowned for their sensitivity to perturbations leading to nonlinear phenomena. A very limited number of papers deal with the study of extreme events in the case of OF,[16,40,41] and, among these papers, conventional OF is sometimes replaced by phase-conjugate feedback[15,42] or filtered OF.[43] So far, none of these studies focused on mid-infrared semiconductor lasers. In the next sections, we pay particular attention to conventional OF in QCLs to retrieve extreme events with, and without, a modulation of the bias current. The distributed feedback QCL under study was manufactured by mirSense. It emits single mode radiation around 5.6 μm with 30-dB side-mode suppression and has a wavelength shift of 20 nm $\cdot$ A^{-1}. The laser is tunable mode-hop free by actuating on the operation temperature and current, with a maximum output power of 50 mW at a cryogenic temperature of 77 K. The device under study was grown by molecular beam epitaxy on an InP cladding and incorporates 30 periods of AlInAs/GaInAs layers.[44] The upper InP cladding is n-doped at a value of 10^{17} cm^{-3} to get electrical injection but without introducing any plasmonic effects. The design for the distributed feedback laser uses an index coupling and metal grating, as previously reported.[45,46] This enables single-mode emission using a top metal grating with a coupling efficiency of $\kappa \approx 4$ cm^{-1}. For the 2-mm long QCL under study in this article, the obtained κL is thus close to unity. The laser emits a continuous wave due to a standard double trench configuration without iron-doped indium phosphide regrowth. The combination of the top metal grating approach and the double trench configuration ensures a stable and reproducible process. The back-facet of this QCL has a high-reflectivity coating (>95%), while the front facet is left as-cleaved. The setup we used in this experimental work is exactly the same as that widely described in Ref. 28 and is recalled in Fig. 1. The sine wave modulation is, however, not always used in this experimental work and may be replaced by an asymmetric square wave with a duty cycle of 20%, meaning that the upper part of the square signal only lasts for one-fifth of the total period. As explained in the next sections, extreme events are more likely to appear when the amplitude of the modulation is weak. Except for the first figure where extreme events are not displayed, the amplitude of the modulation will be limited to 5 mA, corresponding to <2% of the threshold current of the QCL, the latter also being identical to the one used for the entrainment phenomenon study.

3 Results

3.1 Extreme Events in QCLs

QCLs have been proven to output chaotic patterns when OF is applied to them.[27] Further tuning of the spiking dynamics is possible through a sine wave modulation of the pumping current. In this case, the chaotic dropouts synchronize with the periodic modulation, and the number of spikes per periods can vary through a modification of the amplitude of the modulation or the frequency of the modulation.[28] Analyzing the spiking dynamics showed that some configurations led to spikes with a magnified amplitude. The amplitude of these spikes is very sensitive to any change of the parameters, as shown in Fig. 2(b), where a modulation frequency of 2 MHz leads to spikes with an amplitude comparable with that of the sine modulation. A slight change in the frequency of the modulation annihilates the magnified spikes, as can be seen in Figs. 2(a) and 2(c) for a modulation frequency of 1.8 and 2.2 MHz, respectively. In this configuration, the amplitude of the modulation corresponds to 28% of the pumping current. Even in the case of Fig. 2(b), the spikes with a large amplitude cannot be considered as extreme because they do not meet the aforementioned requirements, namely criterion C_1 and criterion C_2. As extreme events are compared with the mean value and the standard deviation of the signal, decreasing the amplitude of the modulation or even suppressing the external modulation is one of the key features to trigger events with a large amplitude compared to the common values of the signal. Figure 3(a) shows a time trace with extreme events when no external modulation is applied. This case differs from the usual configuration where OF gives rise to deterministic chaos because the external cavity is asymmetric, or, in other words, the feedback mirror is a little bit tilted. The backreflected light consequently hits the emission facet of the QCL and, thus, the waveguide imperfectly. It is relevant to notice that variations of the nonlinear dynamics in diode lasers due to a mirror tilt were already studied more than 30 years ago.[47] The authors had also envisioned new types of dynamics and potential applications.

Events surging above the red dashed line and the green dashed line in Fig. 3(a) correspond to extreme events according to criterion C_1 and criterion C_2, respectively. In the following, we focus on the C_1 criterion because its lower threshold allows us to take more extreme events into account. This helps us in providing relevant statistics for the analysis of the retrieved extreme events. Figure 3(b) shows that the time interval between the extreme events is not easily foreseen, and this characteristic is also found in various schemes with extreme pulses. This configuration without modulation of the pump current is thus not optimized for the triggering of extreme events. Indeed, it is not possible to predict when they will pop up, and this prevents any possible utilization of these sudden bursts. Figure 4 gathers the statistics of the intensity of the spikes found in the waveform. The observation time was chosen as a compromise between the

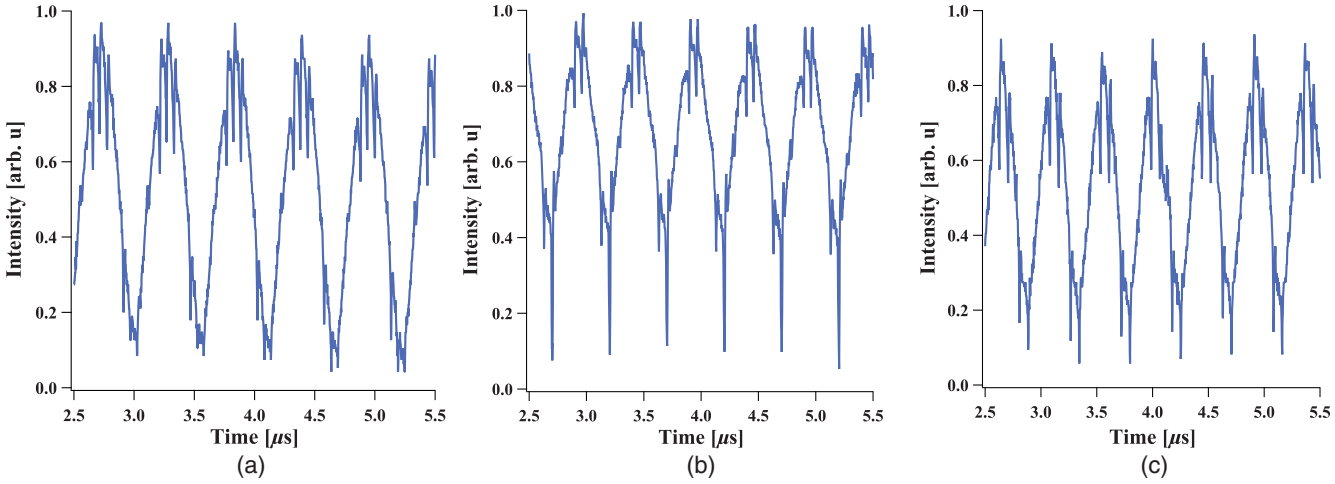

Fig. 2 Experimental time traces of the QCL output when external OF is applied to the QCL and with a sine modulation of the continuous bias of: (a) 1.8 MHz, (b) 2 MHz, and (c) 2.2 MHz; all of the traces were retrieved for a continuous bias of 430 mA and a modulation amplitude of 120 mA, but only the one in the middle exhibits dropouts with a magnified amplitude, which is, however, not enough to categorize them as extreme events.

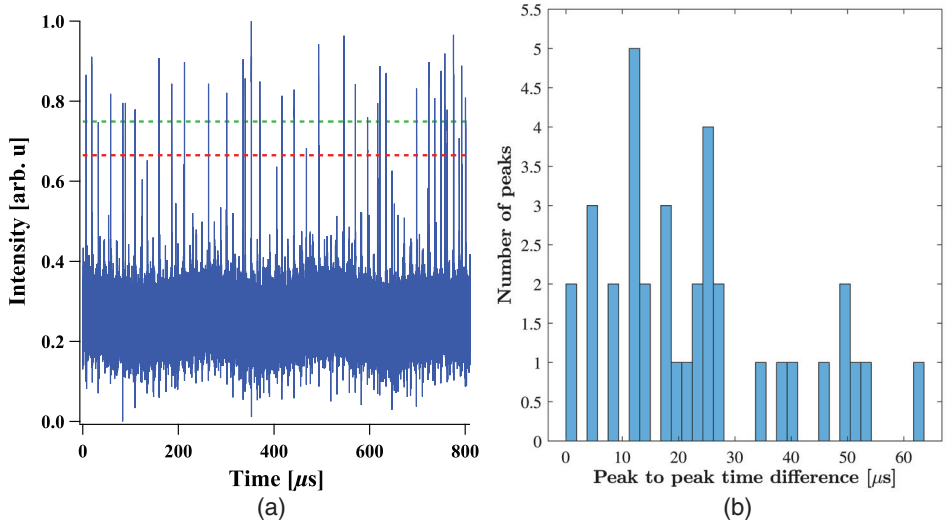

Fig. 3 (a) Experimental time trace with extreme events and associated thresholds for the two criteria. The dashed red line represents the threshold corresponding to criterion C_1 ($H = 0.665$) and the dashed green line represents the threshold corresponding to criterion C_2 ($H = 0.749$). Events with their maximum above these dashed lines are considered as extreme. (b) Histogram of the time intervals between extreme events in the case where the C_1 criterion is applied to the time trace.

number of displayed extreme events and a sufficient resolution to ensure that the retrieved events were not artifacts. There is a clear long-tail distribution in the statistics, which is incompatible with a regular distribution of maxima, and this means that events with a large amplitude appear more frequently than expected. This configuration is very similar to that when studying deterministic chaos in QCLs. Indeed, OF can lead to LFFs[27] but they are mostly unpredictable, which is not the case when a periodic external modulation allows synchronizing the spiking dynamics.[28] Consequently, applying a periodic modulation with a low amplitude is one of the levers to display large events while maintaining the entrainment phenomenon.

3.2 Prediction of Extreme Events in QCLs

Some applications, such as optical neuron-like systems, require optical bursts to be triggered in response to a perturbation. Within other scientific areas, many efforts have also tried to forecast abnormal and striking events, for instance, in medicine,[48] finance,[49] road traffic,[50] or climate science.[51] Extreme

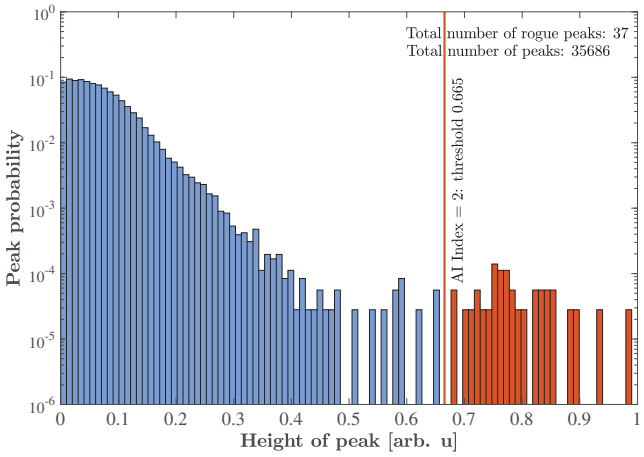

Fig. 4 Histogram of the retrieved maximal intensity and the related threshold for the C_1 criterion. Red bars display the extreme events of the time trace displayed in Fig. 3.

events may also be suppressed in cases where the sudden surge can lead to the destruction of a component, or when it can disrupt the transmission of a private message. This inhibition process is also of prime interest for neuromorphic schemes to interrupt regular trains of bursts.[52,53] Methods to prevent extreme events from occurring have been numerically tested for both the configuration with optical injection[35] and the configuration with OF.[40] For instance, extreme events can be anticipated by studying precursors in the time traces. In the case of a laser diode subject to injection, oscillations emerge during a few nanoseconds before the burst of the spike, which itself lasts <1 ns. In the case of feedback, another pattern is very likely to occur before an extreme event, and the electrical signal can thus be antisynchronized in advance,[54] even if the timescales of the order of nanoseconds are quite challenging in the case of laser diodes. Similarly, an external modulation with an adequate range of frequency and amplitude parameters,[18] or a high level of noise,[35] can suppress extreme events in configurations that were supposed to be prone to such events. The last two mentioned methods were not implemented in our experiments, but the extreme events displayed in QCLs seem to have a characteristic signature, which can be easily forecast because of its large timescale. Figure 5(a) shows the temporal superposition for the 37 extreme events retrieved in the previous section when C_1 criterion is applied. Two main indications can be seen in this figure when focusing on the average of the time traces: a trough occurs ~300 ns before the extreme event happens, and this event is followed by an oscillation lasting a few microseconds with a decreasing amplitude. To draw a comprehensive comparison with the numerical studies,[35,40] we also display the same superposition diagram but for a higher C_1 threshold (abnormality $A = 2.4$) in Fig. 5(b), taking into account 13 extreme events instead of 37. Contrary to the aforementioned simulations, increasing the threshold for giant pulses does not allow us to more clearly predict extreme events, even if the dip following the events is more clearly depicted in the second case. Globally, the oscillation pattern following the spike is more visible in the case where the threshold was lower. Therefore, all of the extreme events, even those that are not that tremendous, can be predicted and potentially suppressed before they occur. We did not try to implement the latter method, but the large elapsed time between the precursor and the spike (a few hundred times larger than that observed with VCSELs or laser diodes) would ease such suppression in the case of unwanted extreme events, as already envisioned in the case of a solid-state laser with an electro-optical modulator.[55] We have to keep in mind

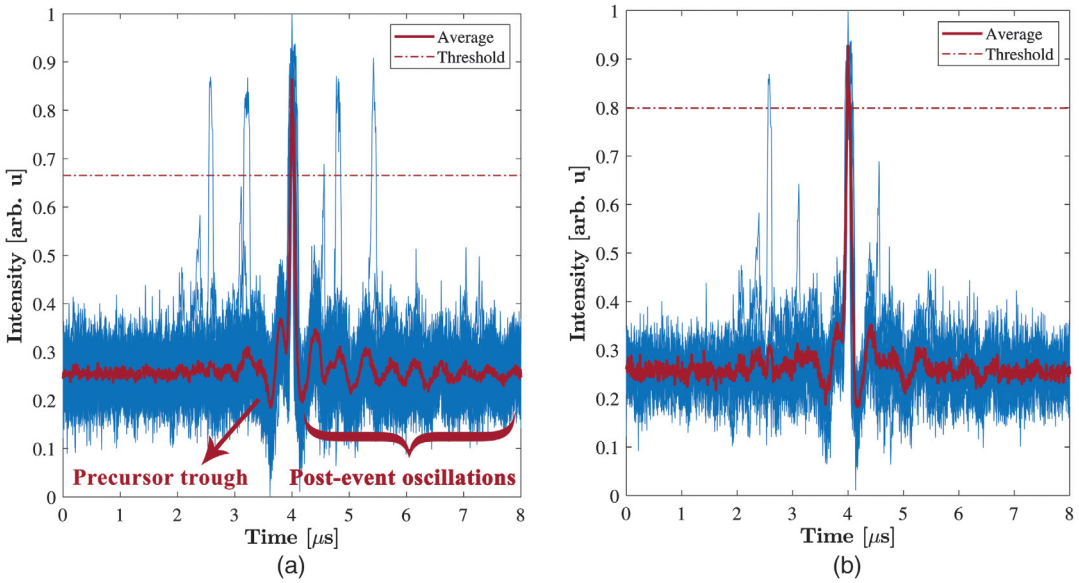

Fig. 5 (a) Time series centered on the maximum of local bursts and superposition of 37 extreme events. The corresponding averaged output power is displayed with a purple solid line and the threshold corresponding to an abnormality of 2 is displayed with a dash-dot line. (b) Same data plot but for 13 extreme events surging above an abnormality index of 2.4. In the left panel, the trough preceding the optical burst, as well as the oscillations following the extreme event, is underlined.

that extreme events can affect the performances of QCLs, and that methods have successfully been tested in other semiconductor lasers to get rid of them. An accurate cartography of the extreme event phenomenon in QCLs would also be useful to determine the impact of several parameters such as the modulation frequency or the value of the spontaneous emission factor.

3.3 Excitability of Extreme Pulses in QCLs

In this section, we focus on excitability in QCLs and on levers to trigger this phenomenon. Extreme events are not easy to predict <1 μs in advance, as we saw in the previous section, and are consequently difficult to monitor. In this section, we show how to experimentally trigger extreme pulses with a probability higher than 40%. Following the conclusions in the first subsection, applying a modulation with a low amplitude will decrease the main value and standard deviation of the laser's output and may be prone to extreme events. Figure 6 shows extreme events appearing when a sine modulation of 0.1 MHz at a low amplitude of 4 mA is applied to the QCL. Criteria C_1 and C_2 are still drawn with red and green dashed lines, respectively. The waveform looks very similar to the one in Fig. 3(a), with extreme events seemingly distributed in a random manner. However, a more accurate analysis of the distribution shows that extreme events can only occur when the external sine modulation reaches a maximum. This is shown in Fig. 6(b) for two extreme events, and this configuration shares similarities with the entrainment phenomenon case at 2 MHz [Fig. 2(b)], where the magnified events were only popping up for a specific phase shift of the modulation signal. This result echoes the microsecond excitability process described in Ref. 56 for a laser diode with stochastic resonance, except that in our case the amplitude of the extreme events is not consistent throughout the time trace. Even if applying a sine modulation allows us to forecast the extreme events in a narrow time interval around the extrema, the maximum success rate is very low (around 10%), and the global picture is that the triggering of these events is almost random. Furthermore, the amplitude of the extreme spikes is not constant throughout the time trace, and this may not be suitable for applications such as neuromorphic photonics.

Sine modulation is, however, not the only lever to trigger extreme events in semiconductor lasers. A recent numerical study showed that the best success rate for triggering such events was obtained when the excitation was a pulse-up signal[39] in the case of an optically injected laser diode. In this configuration, the authors achieved a success rate of 50%. We thus decided to implement a similar pulse-up configuration in the case of OF by means of an asymmetric square wave modulation. This square signal has a duty cycle of 20% and a low amplitude of 4 mA. The period of the pattern is 10 μs. Figure 7(a) shows a time trace of the QCL operated under the aforementioned conditions. Extreme events can only appear simultaneously with the pulse up, corresponding to the upper part of the square wave. Figure 7(b) shows the synchronization of the extreme events with the periodic modulation signal and also depicts the difference in amplitude between the extreme spikes and one of the pulse up, which did not give birth to a magnified event. The latter case is, however, less frequent than in the configuration with a low-amplitude sine forcing, since the success rate for extreme events is now more than 40%. It is relevant to notice that this success rate is very close to that predicted in the simulations for laser diodes.[39] Further comparisons could be drawn with the laser diode case because QCLs have not been found to exhibit relaxation frequency, and this might favor extreme events operation. Indeed, modulating the laser at a frequency below the relaxation frequency leads to a configuration where extreme events are likely to occur. Conversely, modulating above the relaxation frequency does not ensure a high success rate for extreme events. It is even possible to totally avoid extreme events by modulating at a frequency close to the relaxation frequency,[18] when the semiconductor laser under study exhibits such frequency.

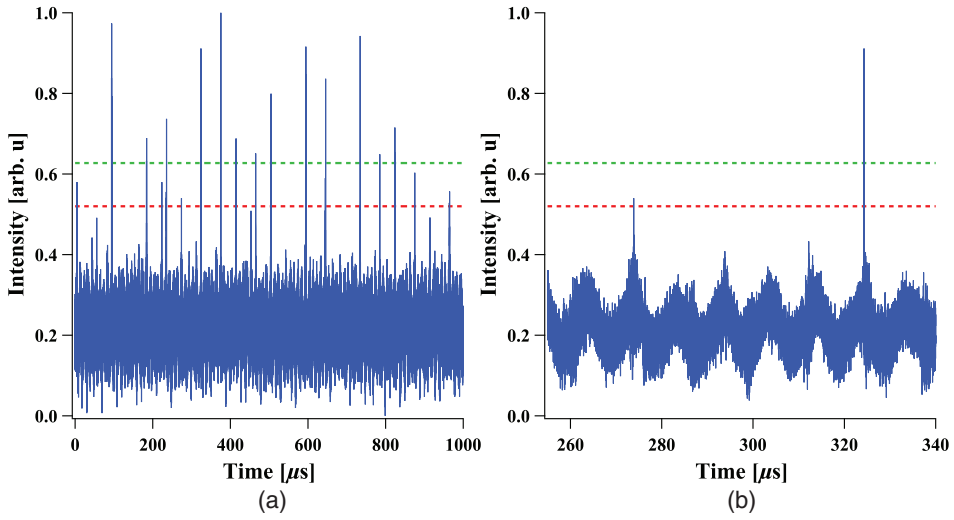

Fig. 6 (a) Experimental time traces of the QCL when OF and a sine wave modulation with a period of 10 μs and an amplitude of 4 mA are applied. The dashed red line represents the C_1 criterion and the dashed green line represents the C_2 criterion. (b) Close-up on extreme events and the low-amplitude sine modulation, revealing that extreme events can only occur on top of the periodic modulation.

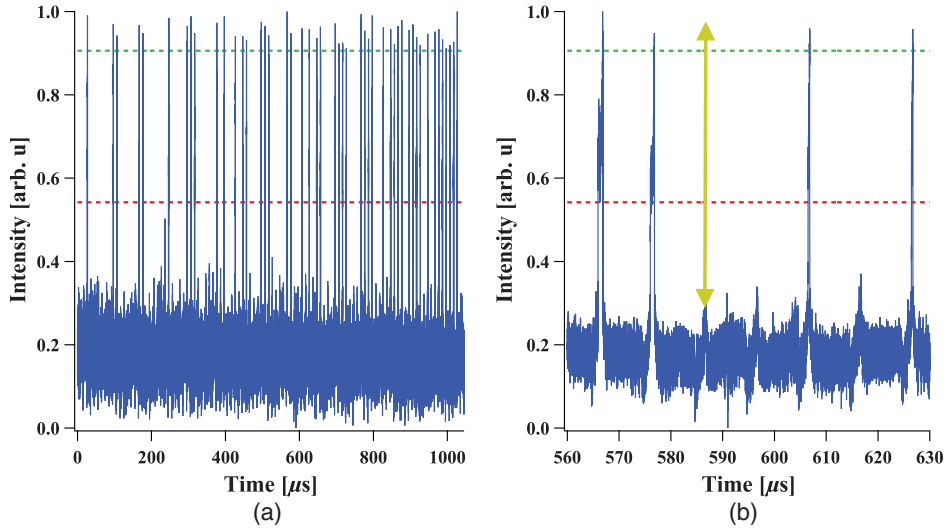

Fig. 7 (a) Experimental time traces of the QCL when OF and an asymmetric square wave modulation with a period of 10 μs, an amplitude of 4 mA, and a duty cycle of 20% are applied. The dashed red line represents the threshold corresponding to criterion C_1, and the dashed green line represents the threshold corresponding to criterion C_2. (b) Close-up on four extreme events and the low-amplitude square modulation, the golden arrow represents the amplitude discrepancy between the extreme pulses and the square wave modulation. Extreme events are synchronized with the pulse up of the perturbation.

The comparison can be extended to the case of VCSELs. For instance, the maximum success rate of 47% that we were able to reach is in good agreement with experiments using pulse-up configurations, since results showed a maximum value of 60%.[36] Similarly to the latter case with VCSELs, the extreme events we were able to produce with a high success rate have an almost constant amplitude, which is consistent with a neuromorphic model. Figure 8 underlines that the time interval between the extreme spikes in the case of Figs. 6 and 7 is given by an integer multiple of the period of the external modulation, which is 10 μs in both configurations. In the case of Fig. 8(a), some integer multiples are more likely to be selected (especially 40, 50, and 90 μs), whereas some others never occur. The extreme events phenomenon seems to be dependent on a parameter of the system, but the long time scale (a few dozens of μs) does not correspond to the external cavity period (which is only

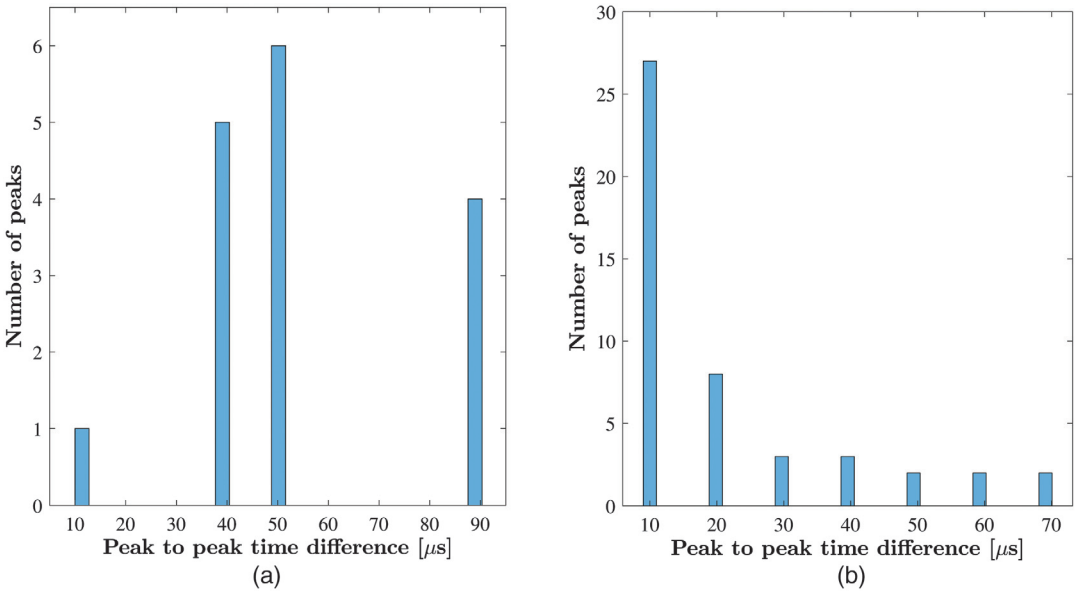

Fig. 8 (a) Histogram of the time intervals between extreme events in the case where C_1 criterion is applied to the time trace of Fig. 6; (b) histogram of the time intervals between extreme events in the case where C_1 criterion is applied to the time trace of Fig. 7.

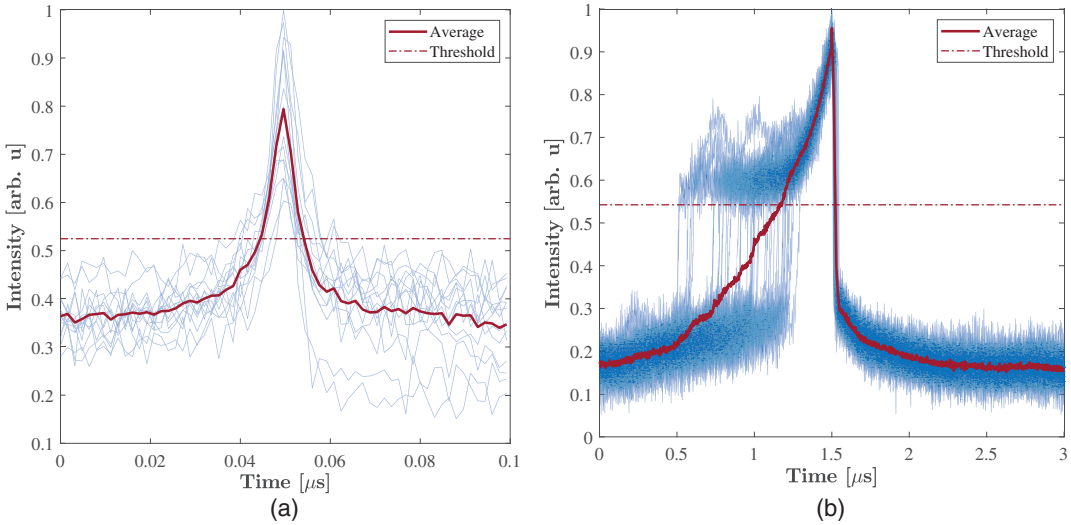

Fig. 9 (a) Time series centered on the maximum of local bursts and superposition of 17 extreme events in the case of the sine perturbation. The corresponding averaged output power is displayed with a purple solid line, and the threshold corresponding to an abnormality index of 2 is displayed with a dash-dot line. (b) Same data plot but for 48 extreme events in the case of the pulse-up perturbation. In the first case, the amplitude of the spikes is not constant, and they are all within a time window of 0.02 μs. In the second case, the spikes have a consistent amplitude but a strong jitter occurs, with a burst width between 0.3 and 1 μs.

a few ns) that is usually responsible for a repetition pattern in the case of phase-conjugate feedback.[15] In the case of Fig. 8(b), most of the extreme events are triggered every 10 μs, corresponding to the period of the external modulation. This eases the potential use of such on-demand bursts for neuron-like systems.

To further analyze the extreme events we triggered, we decided to superimpose the time traces at the peak of the extreme pulse, like we already did in the section dealing with prediction of extreme events. The results show that there is a huge difference between the sine perturbation and the pulse-up perturbation, as can be visualized in Fig. 9. In the case of the pulse-up perturbation, no oscillations can be spotted after the extreme events. Another difference between the several configurations studied is the width and shape of the extreme pulse. A closer look at the pattern obtained in the case of a sine perturbation [Fig. 9(a)] shows that the burst lasts on average 20 ns. In the case of the pulse-up perturbation, Fig. 9(b) shows that the extreme pulse lasts an average of 500 ns and is composed of a large incline followed by a very steep dropoff, simultaneously with the end of the 2-μs square-pattern modulation. It is relevant to notice that, in the context of VCSELs, various patterns of extreme pulses have already been observed while varying the conditions of operation.[36] Indeed, in the case where the injection phase-jump is replaced by a pulse-up similar to the one we applied to the QCL, the VCSEL can generate extreme events lasting $\sim$1 ns, which is almost 10 times longer than those triggered with the phase-jump configuration. Furthermore, the pulse-up also seems to suppress the dip that usually follows extreme events because of the strong linear response the pulse-up produces.[36] Another conclusion of this experimental effort is that the injection configuration allows the authors to reach a maximum success rate (nearly 100%) higher than the pulse-up configuration (roughly 60%). The latter being compatible with the success rate (47%), we were able to achieve in the case of QCLs. Further investigation is required to fully understand how the shape of the extreme events varies with all the parameters we studied in the case of QCLs under OF.

4 Extreme Events for Neuron-Like Systems

Many trials have been carried out in several fields to reproduce the behavior of neurons. Some of the first attempts were performed with chemical oscillators,[57] but the typical characteristic time of nonlinear chemical dynamics is, at least, in the order of seconds[58] and is thus slower than a biological neuron cluster. The electrical domain then drove attention,[59] with complex grids and operation speeds below 1 ms, which is up to 100 times faster than conventional neurons. In order to obtain a faster process, optical neurons have also been considered[60] with many configurations based on VCSEL as the core component[61] and for several experimental activation schemes such as polarization switching,[62] electrical bias stimulation,[63] or via saturable absorber.[64] With VCSELs, the maximum processing rate is close to the GHz and is thus several orders of magnitude faster than the best performances with electrical circuits.[53] The purpose of neuromorphic computing systems is to process information tasks inspired by the brain's powerful computational abilities with ultrafast lasers. One of the key requirements to replicate biological neurons' response is to perform controllable inhibition and excitation (or activation).[65] The latter is fragmented in several subcategories called tonic spiking, phasic spiking, tonic bursting, phasic bursting, excitability, spike thresholding, and spike latency, among others.[66] While most of these subcategories have already been successfully assessed in the case of VCSELs,[53] we demonstrate that tonic spiking, phasic spiking, and spike thresholding can be achieved in a QCL under OF, as illustrated in the following.

In the case of QCLs, we were able to trigger spikes in two different configurations. The one with the sine forcing allowed us to display spikes with a low success rate and with uneven amplitude. Consequently, it would be difficult to take advantage of this process to create an optical neuron, since the two key parameters for such a configuration are high reproducibility and a constant amplitude that does not depend on the excitation strength, provided that this excitation reaches a threshold. The second configuration we tested, with the pulse-up excitation, showed an improved success rate and a consistent amplitude when extreme events are triggered. The conclusion is that the latter configuration is more appropriate for neuromorphic photonics. In order to go a step beyond in the analysis of our two configurations leading to controllable extreme events, we draw a comparison with existing analyses in other semiconductor lasers. The long-tail PDF that we are able to retrieve in the sine modulation case is an indicator that the pulse amplitude displays non-Gaussian features, although a thorough mathematical analysis would be required to claim that the extreme events we observe are rogue waves. This conclusion is also true for the extreme events we were able to display without periodic modulation. The case where all of the extreme events have the same amplitude is a bit different; some experimental results in domains as varied as coupled chaotic oscillators[2] or rainfall statistics[67] have been referred to as dragon-king events. These events do not have the same formation mechanism because they are not scale-free, meaning that giant events are not caused by the same dynamical mechanisms governing the occurrence of small and intermediate events, and this is the reason why giant pulses are favored in comparison with intermediate pulses. However, dragon-king events have been described for configurations without excitation, and we thus do not consider that this terminology can be applied to what we observe with the pulse-up operation. A closer look at the extreme spikes we triggered [Fig. 9(b)] shows that these bursts start with a very steep edge, then are followed by a large incline up to the maximum amplitude, which is itself followed by an abrupt edge down to the free-running value. For all of the extreme bursts, the width of the described process can range from 0.3 to 1 μs, but it is not identical for all the spikes. These three steps are very similar to what has been observed in the case of optical systems under either injection or OF when applying the van der Pol–Fitzhugh–Nagumo (VdPFN) model,[68] consisting in a general scenario of relaxation oscillations that are characterized by the competition of two timescales: the timescale of carriers in the nanosecond range and a thermal timescale in the microsecond range, for a configuration with quantum dot lasers, which are highly damped semiconductor lasers.[69,70] In particular, Ref. 69 also showed spikes with regular amplitude and similar sharp edges. Furthermore, a jitter is also present in the superposition diagram, even though, in the case of quantum dots, the maximum of the burst occurs at the beginning of the pattern, while it occurs at the end of the pattern in our case. In addition, the characteristic time of the pattern observed with quantum dots is very similar to the one we observed with the QCL under OF. The VdPFN model could thus explain why the typical time-delay dynamics, in the range of nanoseconds, observed in other semiconductor laser configurations is not reproduced in our case. Last but not least, the VdPFN model has been recently studied to draw a qualitative comparison between semiconductor lasers with external OF and biological neurons simulated with a stochastic model.[71]

If we have a closer look at our configuration with QCLs, for each occurrence, the spike has a characteristic time in the order of microseconds, and that is of paramount importance in neuromorphic photonics. This indeed means that our basic optical neuron system operates 10,000-times faster than biological neurons and 100-times faster than electronic artificial neurons. Compared with existing optical neuromorphic systems that use semiconductor lasers under the optical injection of a remote laser, our configuration takes advantage of external OF, and, consequently, only one laser component is required to build one basic spiking neuron. This means that excitable QCLs under OF have a response time that bridges the ultrafast neuromorphic optics obtained with VCSELs (characteristic time in the order of nanoseconds) and the electrical neural grids with a characteristic time around the millisecond. Up to date, electrical networks are more complex with configurations made of thousands of neurons, and further inquiries in the case of QCLs and photonics will be dedicated to the combination of several optical neurons to build clusters.[72] The advantage of our OF configuration is that only one laser is required to process a neuron, whereas the optical injection configuration, widely used in VCSELs, requires two lasers. Another drawback of the injection operation is that during the perturbation process, the wavelength of the remote laser is modified, and, consequently, the injection locking is momentarily lost.[63] This means that the wavelength detuning between the master VCSEL and the slave VCSEL must be tuned adequately to have proper operation, and this adds constraints to the conditions of operation. Finally, mid-infrared wavelengths around 6 μm are in the amide-I band and the amide-II band of proteins,[73] which means that these wavelengths are strongly absorbed by biological tissues and are adequate for precise targeting with low collateral damage, especially in neural tissues. Consequently, surgery applications such as coagulation and ablation have already been demonstrated with QCLs emitting at such wavelengths.[74] This paves the way for direct interactions between biological matter and optical neurons based on mid-infrared QCLs within the amide-I and amide-II bands.

5 Conclusion and Perspectives

We experimentally reported on the first observation of extreme pulses in a mid-infrared emitting QCL, and we described a method to trigger them on-demand with a high success rate. Even though it is possible to exhibit extreme events in the case of a free-running QCL with external OF, these events are more likely to happen in a configuration with a periodic modulation of the pumping current and a small amplitude. A fine tuning of the modulation pattern and frequency allows us to control the time interval between the spikes. Although QCLs are not as prone to all-optical pulses and patterns generation, a challenge that was addressed recently in a low-speed configuration,[75] we propose a method to display microsecond pulses with consistent amplitude. These triggered pulses are of paramount importance for neuromorphic systems. With our configuration, we were able to build a basic neuron, and its behavior was in accordance with features found in biological neurons, such as thresholding, phasic spiking, and tonic spiking. Having a global picture about the triggering of extreme events and about the entrainment phenomenon is also essential when it comes to realizing a private transmission using two QCLs. The transmission is actually secure because the message to be transmitted is hidden within the chaotic pattern, and this message is to be recovered due to a

chaos synchronization. However, if the chaotic pattern is disturbed by, for instance, extreme events, the synchronization can be jammed or, even worse, the message can become obvious among the chaotic carrier. The privacy of the message would consequently be broken. This can be considered a serious threat because encoding a message introduces specific frequencies in the electrical signal driving the QCL and may lead to extreme events synchronized with the pulse-up. A thorough analysis of the amplitude and frequency of the message is necessary to minimize such drawbacks. Further analysis will also consider development of strong numerical modeling incorporating the QCL features to better understand the mechanisms driving the formation of extreme events in such gain media. It could also be of prime interest to trigger the spiking neurons not with a purely electrical excitation, but with a square pattern produced by another QCL under OF to build an all-optical neuromorphic system. This is the subject of ongoing work and will be reported in due course.

Acknowledgments

Authors acknowledge Zhangji Zhao for assistance in the cryogenic measurements, Prof. Cristina Masoller as well as Prof. Benjamin S. Williams, Dr. Sudeep Khanal, Dr. Christopher Curwen, and Albert Demke for the fruitful discussions. This work was supported by the French Defense Agency (DGA), the French ANR program (ANR-17-ASMA-0006), the European Office of Aerospace Research and Development (FA9550-18-1-7001), the Office of Naval Research (N00014-16-1-2094), and the National Science Foundation (DMR-1611598). The authors declare that there are no conflicts of interest related to this article.

References

1. A. Toffoli et al., "Occurrence of extreme waves in three-dimensional mechanically generated wave fields propagating over an oblique current," *Nat. Hazards Earth Syst. Sci.* **11**(3), 895–903 (2011).
2. H. L. D. S. Cavalcante et al., "Predictability and suppression of extreme events in a chaotic system," *Phys. Rev. Lett.* **111**(19), 198701 (2013).
3. T. C. Peterson, P. A. Stott, and S. Herring, "Explaining extreme events of 2011 from a climate perspective," *Bull. Am. Meteorol. Soc.* **93**(7), 1041–1067 (2012).
4. N. S. Frolov et al., "Statistical properties and predictability of extreme epileptic events," *Sci. Rep.* **9**(1), 7243 (2019).
5. S. Bialonski, G. Ansmann, and H. Kantz, "Data-driven prediction and prevention of extreme events in a spatially extended excitable system," *Phys. Rev. E* **92**(4), 042910 (2015).
6. N. Akhmediev et al., "Roadmap on optical rogue waves and extreme events," *J. Opt.* **18**(6), 063001 (2016).
7. C. Bonatto et al., "Deterministic optical rogue waves," *Phys. Rev. Lett.* **107**(5), 053901 (2011).
8. D. Solli et al., "Optical rogue waves," *Nature* **450**(7172), 1054–1057 (2007).
9. C. Liu et al., "Triggering extreme events at the nanoscale in photonic seas," *Nat. Phys.* **11**(4), 358–363 (2015).
10. R. Höhmann et al., "Freak waves in the linear regime: a microwave study," *Phys. Rev. Lett.* **104**(9), 093901 (2010).
11. V. Makarov, V. Nekorkin, and M. Velarde, "Spiking behavior in a noise-driven system combining oscillatory and excitatory properties," *Phys. Rev. Lett.* **86**(15), 3431–3434 (2001).
12. E. Viktorov and T. Erneux, "Self-sustained pulsations in a quantum-dot laser," *Phys. Rev. E* **90**(5), 052914 (2014).
13. S.-S. Lin, S.-K. Hwang, and J.-M. Liu, "High-power noise-like pulse generation using a 1.56-μm all-fiber laser system," *Opt. Express* **23**(14), 18256–18268 (2015).
14. A. Montina et al., "Non-Gaussian statistics and extreme waves in a nonlinear optical cavity," *Phys. Rev. Lett.* **103**(17), 173901 (2009).
15. A. K. Dal Bosco, D. Wolfersberger, and M. Sciamanna, "Extreme events in time-delayed nonlinear optics," *Opt. Lett.* **38**(5), 703–705 (2013).
16. D. Choi et al., "Low-frequency fluctuations in an external-cavity laser leading to extreme events," *Phys. Rev. E* **93**(4), 042216 (2016).
17. M. G. Kovalsky, A. A. Hnilo, and J. R. Tredicce, "Extreme events in the Ti: sapphire laser," *Opt. Lett.* **36**(22), 4449–4451 (2011).
18. S. Perrone et al., "Controlling the likelihood of rogue waves in an optically injected semiconductor laser via direct current modulation," *Phys. Rev. A* **89**(3), 033804 (2014).
19. R. Karnatak et al., "Route to extreme events in excitable systems," *Phys. Rev. E* **90**(2), 022917 (2014).
20. O. Spitz et al., "Low-frequency fluctuations of a mid-infrared quantum cascade laser operating at cryogenic temperatures," *Laser Phys. Lett.* **15**(11), 116201 (2018).
21. J. Faist et al., "Quantum cascade laser," *Science* **264**(5158), 553–556 (1994).
22. M. S. Vitiello et al., "Quantum cascade lasers: 20 years of challenges," *Opt. Express* **23**(4), 5167–5182 (2015).
23. H. D. Tholl, "Review and prospects of optical countermeasure technologies," *Proc. SPIE* **10797**, 1079702 (2018).
24. X. Pang et al., "Gigabit free-space multi-level signal transmission with a mid-infrared quantum cascade laser operating at room temperature," *Opt. Lett.* **42**(18), 3646–3649 (2017).
25. A. G. Davies et al., "Terahertz spectroscopy of explosives and drugs," *Mater. Today* **11**(3), 18–26 (2008).
26. A. W. Lee et al., "Real-time terahertz imaging over a standoff distance (>25 meters)," *Appl. Phys. Lett.* **89**(14), 141125 (2006).
27. L. Jumpertz et al., "Chaotic light at mid-infrared wavelength," *Light Sci. Appl.* **5**(6), e16088 (2016).
28. O. Spitz et al., "Chaotic optical power dropouts driven by low frequency bias forcing in a mid-infrared quantum cascade laser," *Sci. Rep.* **9**(1), 4451 (2019).
29. N. Yu et al., "Coherent coupling of multiple transverse modes in quantum cascade lasers," *Phys. Rev. Lett.* **102**(1), 013901 (2009).
30. A. K. Wójcik et al., "Self-synchronization of laser modes and multistability in quantum cascade lasers," *Phys. Rev. Lett.* **106**(13), 133902 (2011).
31. S. Sauvage et al., "Third-harmonic generation in InAs/GaAs self-assembled quantum dots," *Phys. Rev. B* **59**(15), 9830–9833 (1999).
32. P. Friedli et al., "Four-wave mixing in a quantum cascade laser amplifier," *Appl. Phys. Lett.* **102**(22), 222104 (2013).
33. A. Delga and L. Leviandier, "Free-space optical communications with quantum cascade lasers," *Proc. SPIE* **10926**, 1092617 (2019).
34. K. Schires et al., "Rare disruptive events in polarisation-resolved dynamics of optically injected 1550 nm VCSELs," *Electron. Lett.* **48**(14), 872–874 (2012).
35. J. Zamora-Munt et al., "Rogue waves in optically injected lasers: origin, predictability, and suppression," *Phys. Rev. A* **87**(3), 035802 (2013).
36. M. Turconi et al., "Control of excitable pulses in an injection-locked semiconductor laser," *Phys. Rev. E* **88**(2), 022923 (2013).
37. A. Hurtado and J. Javaloyes, "Controllable spiking patterns in long-wavelength vertical cavity surface emitting lasers for neuromorphic photonics systems," *Appl. Phys. Lett.* **107**(24), 241103 (2015).
38. N. M. Alvarez, S. Borkar, and C. Masoller, "Predictability of extreme intensity pulses in optically injected semiconductor lasers," *Eur. Phys. J. Spec. Top.* **226**(9), 1971–1977 (2017).
39. T. Jin, C. Siyu, and C. Masoller, "Generation of extreme pulses on demand in semiconductor lasers with optical injection," *Opt. Express* **25**(25), 31326–31336 (2017).

40. J. A. Reinoso, J. Zamora-Munt, and C. Masoller, "Extreme intensity pulses in a semiconductor laser with a short external cavity," *Phys. Rev. E* **87**(6), 062913 (2013).
41. C.-H. Uy, D. Rontani, and M. Sciamanna, "Vectorial extreme events in VCSEL polarization dynamics," *Opt. Lett.* **42**(11), 2177–2180 (2017).
42. É. Mercier et al., "Numerical study of extreme events in a laser diode with phase-conjugate optical feedback," *Phys. Rev. E* **91**(4), 042914 (2015).
43. M. W. Lee et al., "Demonstration of optical rogue waves using a laser diode emitting at 980 nm and a fiber Bragg grating," *Opt. Lett.* **41**(19), 4476–4479 (2016).
44. A. Evans et al., "High-temperature, high-power, continuous-wave operation of buried heterostructure quantum-cascade lasers," *Appl. Phys. Lett.* **84**(3), 314–316 (2004).
45. M. Carras et al., "Top grating index-coupled distributed feedback quantum cascade lasers," *Appl. Phys. Lett.* **93**(1), 011109 (2008).
46. M. Carras et al., "Room-temperature continuous-wave metal grating distributed feedback quantum cascade lasers," *Appl. Phys. Lett.* **96**(16), 161105 (2010).
47. J.-D. Park et al., "Low-frequency self-pulsations in asymmetric external-cavity semiconductor lasers due to multiple-feedback effects," *Opt. Lett.* **14**(19), 1054–1056 (1989).
48. J. Martinerie et al., "Epileptic seizures can be anticipated by nonlinear analysis," *Nat. Med.* **4**(10), 1173–1176 (1998).
49. J. Feigenbaum, "Financial physics," *Rep. Prog. Phys.* **66**(10), 1611 (2003).
50. N. Laptev et al., "Time-series extreme event forecasting with neural networks at Uber," in *Int. Conf. Mach. Learn.*, Vol. 34, pp. 1–5 (2017).
51. V. Dakos et al., "Slowing down as an early warning signal for abrupt climate change," *Proc. Natl. Acad. Sci. U. S. A.* **105**(38), 14308–14312 (2008).
52. J. Robertson et al., "Controlled inhibition of spiking dynamics in VCSELs for neuromorphic photonics: theory and experiments," *Opt. Lett.* **42**(8), 1560–1563 (2017).
53. J. Robertson et al., "Toward neuromorphic photonic networks of ultrafast spiking laser neurons," *IEEE J. Sel. Top. Quantum Electron.* **26**(1), 7700715 (2020).
54. J. Zamora-Munt, C. R. Mirasso, and R. Toral, "Suppression of deterministic and stochastic extreme desynchronization events using anticipated synchronization," *Phys. Rev. E* **89**(1), 012921 (2014).
55. N. M. Granese et al., "Extreme events and crises observed in an all-solid-state laser with modulation of losses," *Opt. Lett.* **41**(13), 3010–3012 (2016).
56. F. Marino et al., "Experimental evidence of stochastic resonance in an excitable optical system," *Phys. Rev. Lett.* **88**(4), 040601 (2002).
57. V. K. Vanag et al., "Oscillatory cluster patterns in a homogeneous chemical system with global feedback," *Nature* **406**(6794), 389–391 (2000).
58. F. Sagués and I. R. Epstein, "Nonlinear chemical dynamics," *Dalton Trans.* **7**, 1201–1217 (2003).
59. B. V. Benjamin et al., "Neurogrid: a mixed-analog-digital multichip system for large-scale neural simulations," *Proc. IEEE* **102**(5), 699–716 (2014).
60. E. C. Mos et al., "Optical neuron by use of a laser diode with injection seeding and external optical feedback," *IEEE Trans. Neural Networks* **11**(4), 988–996 (2000).
61. P. R. Prucnal et al., "Recent progress in semiconductor excitable lasers for photonic spike processing," *Adv. Opt. Photonics* **8**(2), 228–299 (2016).
62. A. Hurtado et al., "Investigation of vertical cavity surface emitting laser dynamics for neuromorphic photonic systems," *Appl. Phys. Lett.* **100**(10), 103703 (2012).
63. J. Robertson, E. Wade, and A. Hurtado, "Electrically controlled neuron-like spiking regimes in vertical-cavity surface-emitting lasers at ultrafast rates," *IEEE J. Sel. Top. Quantum Electron.* **25**(6), 5100307 (2019).
64. Y. Zhang et al., "Spike encoding and storage properties in mutually coupled vertical-cavity surface-emitting lasers subject to optical pulse injection," *Appl. Opt.* **57**(7), 1731–1737 (2018).
65. M. A. Nahmias et al., "A leaky integrate-and-fire laser neuron for ultrafast cognitive computing," *IEEE J. Sel. Top. Quantum Electron.* **19**(5), 1800212 (2013).
66. E. M. Izhikevich, "Which model to use for cortical spiking neurons?" *IEEE Trans. Neural Networks* **15**(5), 1063–1070 (2004).
67. D. Sornette and G. Ouillon, "Dragon-kings: mechanisms, statistical methods and empirical evidence," *Eur. Phys. J. Spec. Top.* **205**, 1–26 (2012).
68. F. Marino et al., "Thermo-optical 'canard orbits' and excitable limit cycles," *Phys. Rev. Lett.* **92**(7), 073901 (2004).
69. A. Tierno, N. Radwell, and T. Ackemann, "Low-frequency self-pulsing in single-section quantum-dot laser diodes and its relation to optothermal pulsations," *Phys. Rev. A* **84**(4), 043828 (2011).
70. M. Dillane et al., "Square wave excitability in quantum dot lasers under optical injection," *Opt. Lett.* **44**(2), 347–350 (2019).
71. J. Tiana-Alsina, C. Quintero-Quiroz, and C. Masoller, "Comparing the dynamics of periodically forced lasers and neurons," *New J. Phys.* **21**(10), 103039 (2019).
72. A. Dolcemascolo et al., "Effective low-dimensional dynamics of a mean-field coupled network of slow-fast spiking lasers," *Phys. Rev. E* **101**(5), 052208 (2020).
73. G. Edwards et al., "Tissue ablation by a free-electron laser tuned to the amide II band," *Nature* **371**, 416–419 (1994).
74. Y. Huang and J. U. Kang, "Quantum cascade laser thermal therapy guided by FDOCT," *Chin. Opt. Lett.* **11**(1), 011701 (2013).
75. M. Montesinos-Ballester et al., "Optical modulation in Ge-rich SiGe waveguides in the mid-infrared wavelength range up to 11 μm," *Commun. Mater.* **1**, 6 (2020).

Olivier Spitz received his PhD in electrical engineering from the Université Paris-Saclay, France, in 2019 and is now a postdoctoral researcher with Télécom Paris, working on applications of mid-infrared QCLs. He has been a visiting scholar in the Electrical and Computer Engineering Department at UCLA, USA, and in the Institut für Angewandte Physik at TU-Darmstadt, Germany. His research interests include nonlinear dynamics, free-space communications, and neuromorphic photonics. He is a member of SPIE and OSA.

Jiagui Wu received his MSc degree in optics from Southwest University, Chongqing, China, in 2006. In 2014, he received his PhD in nonlinear dynamics from Sichuan University, Chengdu, China. He is a professor at the College of Electronic and Information Engineering, Southwest University, Chongqing, China, and a visiting scholar in the Electrical and Computer Engineering Department of the University of California Los Angeles, USA. He has coauthored over 60 publications including 40 journal papers.

Andreas Herdt received his BSc degree in physics in 2014 and his MSc degree in physics in 2016 from the Technical University of Darmstadt, Germany. In 2017, he was awarded with the "Green Photonics Award for Young Academic Researchers" from Fraunhofer IOF for the work of his master thesis. He is currently working with the group of Prof. Elsäßer (Technical University of Darmstadt, Germany) toward his PhD.

Grégory Maisons received his PhD in solid-state physics from the University of Grenoble, France, in 2010. He then joined the III-V Laboratory at Alcatel Thales, Palaiseau, France, before becoming principal investigator at mirSense in 2014, where he is especially involved in electron transport and electromagnetics. His interests include mid-infrared and far-infrared quantum cascade lasers and quantum infrared detectors (QWIPs and quantum cascade detectors). He has coauthored over 50 publications including 15 journal papers.

Mathieu Carras received his PhD in solid-state physics from the University of Paris VII, Denis Diderot, France, in 2006. He then joined the III-V Laboratory at Alcatel Thales, Palaiseau, France, as a permanent research staff member working on modeling, design, and characterization of quantum cascade lasers. He is currently the CEO of mirSense, the company he founded in 2014, after being the head of the team developing mid-infrared lasers at the III-V Laboratory.

Wolfgang Elsäßer received his PhD in physics from the University of Stuttgart, Germany, in 1984, and the habilitation degree in experimental physics from the Philipps University of Marburg, Germany, in 1991. Since 1995, he has been a professor at the Institute of Applied Physics, Technische Universität Darmstadt, Darmstadt, Germany, where he is currently the head of the Semiconductor Optics Group. He is a member of the German Physical Society and the European Physical Society.

Chee-Wei Wong examines mesoscale ultrafast, precision, and quantum measurements. He serves as the Tannas Professor of Engineering at the University of California. He is elected into the National Academy of Inventors, a fellow of APS, IEEE, OSA, ASME, and SPIE, and recipient of NIH Early Scientist Trailblazer, DARPA Young Faculty, NSF CAREER, and Google Faculty Awards, among others. He has supervised 38 PhD scientists; about half are now in their own professorships including full professors.

Frédéric Grillot received his PhD in electrical engineering from the University of Besançon, France, in 2003, and the habilitation thesis in physics from the University of Paris VII, France, in 2012. He is currently a full professor at Télécom Paris, France, and a research professor at the University of New-Mexico, USA. He is a fellow member of SPIE, and a senior member of IEEE and OSA.